

CHEMISTRY

A European Journal

A Journal of



Accepted Article

Title: Synthesis of Benzodihydrofurans by Asymmetric C-H Insertion Reactions of Donor/Donor Carbenoids

Authors: Jared Thomas Shaw, Kellan N. Lamb, Richard A. Squitieri, Srinivasa R. Chintala, Ada J. Kwong, Edward I. Balmond, Cristian Soldi, Olga Dmytrenko, Marta Castiñeira Reis, Ryan Chung, J. Bennett Addison, James C. Fettinger, Jason C. Hein, Dean J. Tantillo, and Joseph M. Fox

This manuscript has been accepted after peer review and appears as an Accepted Article online prior to editing, proofing, and formal publication of the final Version of Record (VoR). This work is currently citable by using the Digital Object Identifier (DOI) given below. The VoR will be published online in Early View as soon as possible and may be different to this Accepted Article as a result of editing. Readers should obtain the VoR from the journal website shown below when it is published to ensure accuracy of information. The authors are responsible for the content of this Accepted Article.

To be cited as: *Chem. Eur. J.* 10.1002/chem.201701630

Link to VoR: <http://dx.doi.org/10.1002/chem.201701630>

Supported by
ACES

WILEY-VCH

Synthesis of Benzodihydrofurans by Asymmetric C–H Insertion Reactions of Donor/Donor Rhodium Carbenes

Kellan N. Lamb,^{†∞} Richard A. Squitieri,^{†∞} Srinivasa R. Chintala,[‡] Ada J. Kwong,[†] Edward I. Balmond,[†] Cristian Soldi,[†] Olga Dmytrenko,[‡] Marta Castiñeira Reis,[†] Ryan Chung,[§] J. Bennett Addison,[†] James C. Fettinger,[†] Jason E. Hein,[§] Dean J. Tantillo,[†] Joseph M. Fox,^{*,‡} Jared T. Shaw^{*,†}

[†]Department of Chemistry, One Shields Ave, University of California, Davis, CA, 95616

[∞]These authors contributed equally to this work.

[‡]Department of Chemistry and Biochemistry, University of Delaware, Newark, Delaware 19716, United States

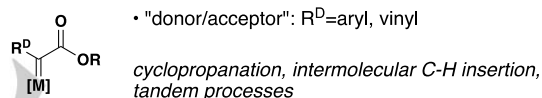
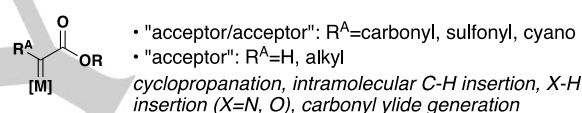
[§]Department of Chemistry, University of British Columbia, Vancouver, British Columbia V6T 1Z1, Canada

Abstract: Metal carbenes appended with two electron-donating groups, known as “donor/donor” carbenes, undergo diastereo- and enantioselective rhodium-catalyzed C–H insertion reactions with ether substrates to form benzodihydrofurans. Unlike the reactions of metal carbenes with electron-withdrawing groups attached, the attenuated electrophilicity enables these reactions to be conducted in Lewis basic solvents (e.g., acetonitrile) and in the presence of water. The diazo precursors for these species are prepared in situ from hydrazone using a mild and chemoselective oxidant (MnO₂). Although this sequence often can be performed in one-pot, control experiments have elucidated why a “two-pot” process is often more efficient. A thorough screen of achiral catalysts demonstrates that sterically-encumbered catalysts are optimal for diastereoselective reactions. Although efficient insertion into allylic and propargylic C–H bonds is observed, competing dipolar cycloaddition processes are noted for some substrates. The full substrate scope of this useful method of benzodihydrofuran synthesis, mechanisms of side reactions, and computational support for the origins of stereoselectivity are described.

Introduction

In the area of enantioselective catalysis, metal-catalyzed C–H insertions are well known as useful and versatile reactions to promote C–C and C–heteroatom bond formation with high levels of selectivity. The bulk of C–H insertion research over the past 30 years has focused on rhodium (II) as an effective catalyst for both inter- and intramolecular reactions. Pioneering work^{1,2} has led to the development of highly effective ligands that have solidly established the utility of rhodium-(II)-catalyzed C–H insertions in organic synthesis³.

Typical metal carbenes



This work

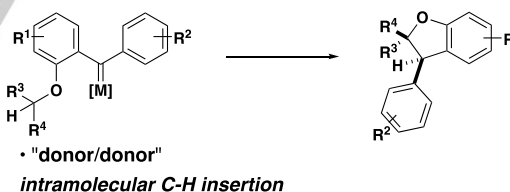


Figure 1. Structure of metal carbenes.

The key intermediate in a C–H insertion is a metal carbene, typically derived from a diazo compound. The reactivity of metal carbenes is controlled by the functional groups adjacent to the carbene center. An electron-withdrawing group, such as a carbonyl, sulfonyl, or cyano is classified as an acceptor, whereas an electron-donating group, such as an aryl or vinyl group, is considered a donor (in a π-sense; Figure 1). Acceptor- and acceptor/acceptor carbene have found great utility in the formation of lactones and cyclic ketones via intramolecular C–H insertion.⁴ However, the high reactivity of acceptor- and acceptor/acceptor carbenes can present challenges for achieving high chemoselectivity in C–H insertion reactions.⁵ When one of the acceptor groups is replaced with a donor group, resulting in a “donor/acceptor” carbene, the reactivity is attenuated, allowing for highly

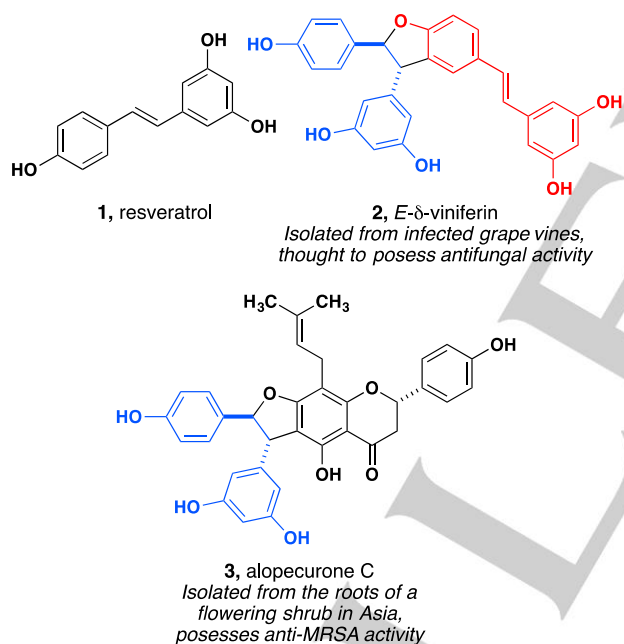
FULL PAPER

WILEY-VCH

selective intermolecular insertions to take place⁶. While C–H insertion reactions have been published extensively for the three aforementioned carbene categories, examples of metal-catalyzed C–H insertion reactions of donor/donor carbene are few^{7,8,9} and no enantioselective reactions were published prior to our first entry into this area¹⁰. Subsequent to our initial report, Fürstner published X-ray crystal structures of several rhodium carbenes, which have helped illuminate the origin of their reactivity.¹¹

We initially explored the C–H insertion reactions of donor-donor carbenes as an entry into the enantioselective synthesis of benzodihydrofurans (BDFs)¹². This heterocyclic core is found widely in natural products, most notably in the oligomers of resveratrol. Resveratrol is a polyphenolic phytoalexin produced by plants in response to infection or injury, often oligomerizing to form complicated structures. Studies suggest that resveratrol itself is partly responsible for the health benefits of drinking red wine¹³, whereas some of the oligomers derived from resveratrol also possess interesting bioactivities (Figure 2).^{14,15}

Figure 2. Target resveratrol-derived molecules featuring benzodihydrofuran and indane core structures.



Resveratrol dimers have been previously accessed through cyclization,¹⁶ metal-catalyzed cross couplings,¹⁷ and enzymatic transformations.¹⁸ Enzymatic transformations are challenging to control for a single target and often provide a complex product mixture. Synthetic methods provide excellent product control, however, much of the work has been focused on carbocycles such as indane and indanones and very little has been done to address heterocyclic targets containing a benzodihydrofuran core. Additionally, none of the synthetic methods applied to resveratrol derivative synthesis are enantioselective. The natural products are isolated as both racemates and single enantiomers, thus there is a need for a robust method to synthesize

enantiomerically pure resveratrol derivatives. We noticed an opportunity to develop the C–H insertion reaction of donor/donor carbenes for application in natural product synthesis. C–H insertion has been previously used in the total synthesis of BDF natural products such as (-)-ephedradine A, (orantine)¹⁹, (-)-serotobenine and (-)-decursivine²⁰, (-)-aperidine²¹, and (+)-lithospermic acid²² (Figure 3). In most cases, enantioselectivity is imparted by both a chiral rhodium catalyst and a chiral auxiliary. The diazo species in all cases is donor/acceptor. While donor-acceptor carbenes have been shown to undergo a wide variety of highly selective intermolecular reactions⁶, these natural product syntheses demonstrate that the selectivities are often lower for intramolecular reactions.

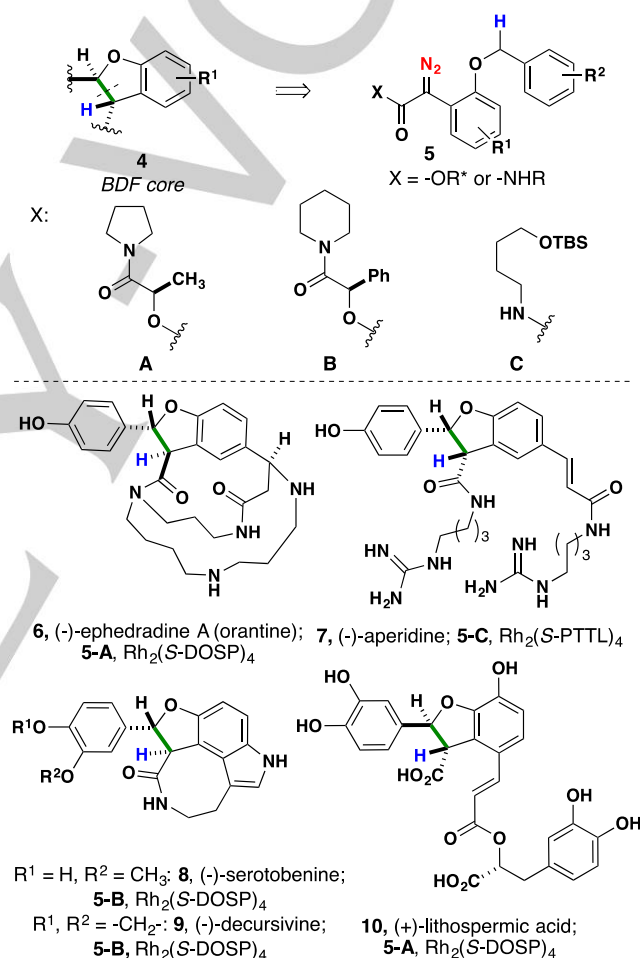


Figure 3. Previous examples of C–H insertion in BDF synthesis.

Recently, we reported our initial study of the intramolecular C–H insertion of donor/donor Rh(II) carbenes¹⁰. Derivatives of 2-hydroxybenzophenone were converted to a diaryl diazo compounds and were effective in forming benzodihydrofurans via C–H insertion. We also demonstrated the utility of our method by synthesizing **2** (Figure 2) for the first time as a single enantiomer. Herein, we report our full study including an expanded scope and exploration of side reactions, as well as mechanistic and kinetic studies.

Table 1. Screening of dirhodium tetracarboxylate catalysts to optimize yield and diastereoselectivity

Symmetrical Catalysts

14, R=CH₃
 15, R=Ph
 16, R=*p*-FC₆H₅

17, R¹=H, R²=F
 18, R¹=H, R²=OCH₃
 19, R¹=R²=H
 20, R¹=R²=CH₃

Unsymmetrical Catalysts

21
 22
 23

24, R¹=CH₃, R²=*p*-FC₆H₄
 25, R¹=Ph, R²=(*o*-CH₃)C₆H₅
 26, R¹=CH₃, R²=Ph
 27, R¹=Et, R²=*i*-Pr

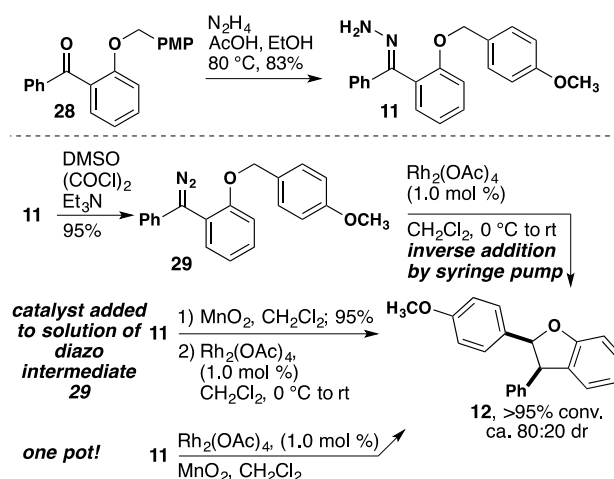
entry	catalyst	12:13	dr	yield (insertion)	entry	catalyst	12:13	dr	yield (insertion)
1	Rh ₂ (OAc) ₄	>95:5	88:12	88%	11	19	>95:5	62:38	68%
2	Rh ₂ (TFA) ₄	>95:5	82:18	65%	12	20	>95:5	94:6	81%
3	Rh ₂ (esp) ₂	59:41	93:7	48%	13	21	60:40	82:18	53%
4 ^a	Rh ₂ (esp) ₂	35:65	90:10	ND ^d	14	22	>95:5	78:22	68%
5 ^b	Rh ₂ (esp) ₂	>95:5	92:8	ND	15	23	>95:5	>95:5	84%
6	14	52:48	84:16	37%	16	24	67:33	92:8	60%
7	15	>95:5	>95:5	79%	17	25	>95:5	>95:5	89%
8	16	>95:5	>95:5	79%	18	26	76:24	93:7	63%
9 ^c	17	ND	53:47	59%	19	27	89:11	>95:5	81%
10 ^c	18	ND	58:42	63%					

^aReaction was run at -20°C; ^bOxidant was filtered prior to catalyst addition; ^cComplex reaction mixture prevented ratio determination; ^dNot determined

Results and Discussion

Method Development. Our initial investigation into the C–H insertion of diaryl Rh(II) carbenes was conducted with diazo **29** (Scheme 1). Initially, diazo compound **29** was prepared and isolated using Swern conditions as reported by Brewer²³. This substrate was added to a solution of Rh₂(OAc)₄ using a syringe pump and produced **12** in high yield and with modest diastereoselection for the syn isomer. After investigating a few other oxidants, MnO₂ emerged as the most operationally simple²⁴. After isolation, a small quantity of Rh₂(OAc)₄ was added to the solution of diazo intermediate **29** and again, high yield for the product was observed. Finally, in an attempt to streamline the process, the oxidant (MnO₂) and catalyst were sequentially added to a solution of the hydrazone, once again resulting in a high level of conversion to the product. With these conditions in hand, we investigated additional achiral rhodium catalysts. Commercially available Rh₂(TFA)₄ and Rh₂(esp)₂ were unable to improve on the preliminary result (Table 1, entries 2 and 3). Initially, we attributed the lower yields to lower catalyst efficiency. Upon closer inspection of the ¹H NMR of the crude reaction, it was clear that in the case of Rh₂(esp)₂ there was a significant byproduct present. Isolation and characterization of this byproduct revealed its identity as imine **13** (Table 1). Subsequent experiments revealed that the formation of imine is increased at lower temperature (Table 1, entry 4) and is negated entirely when the oxidant was filtered away prior to catalyst addition (Table 1, entry 5). To obtain insight in to steric and electronic effects of ligand structure on selectivity for C–H insertion, we

investigated a series of dirhodium carboxylate catalysts, including several catalysts that have not been described previously (Table 1, entries 8, 12, 15, 16, 17, 19). Catalysts with bulky carboxylate ligands, e.g. Rh₂(O₂CPh₃)₄, resulted in excellent diastereoselectivity and yield with no observable imine formation (Table 1, entries 7, 8, 15, 17). Although Rh₂(O₂CPh)₄ (entry 11) gave good



Scheme 1. Initial investigation of diaryl rhodium(II) carbenes in C–H insertion.

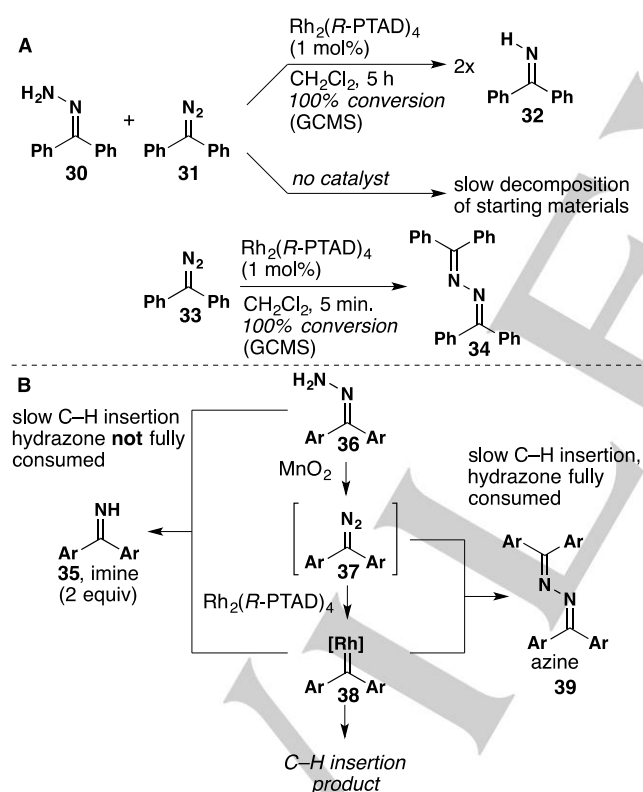
chemoselectivity for C–H insertion, the diastereoselectivity was low and could be improved by replacing the phenyl ring with either mesityl or 9-anthracenyl (Table 1, entries 12 and 15). Alkyl substitutions showed an increased preference for

FULL PAPER

WILEY-VCH

imine formation and generally suffered from lower isolated yields as a result (entries 6, 13, 18 and 19). $\text{Rh}_2(\text{cap})_4$ was a unique catalyst for this screen as the only non-tetracarboxylate ligand and afforded excellent chemoselectivity for C–H insertion, though both the dr and yield were modest (entry 14).

Although imine **13** would appear to be a product of hydrogenolysis of the hydrazone, the oxidative nature of the reaction conditions ruled out this pathway. A control experiment with benzophenone hydrazone **30** suggests that the imine is a product of hydrazone reacting with carbene. When a mixture of hydrazone (30) and diphenyldiazomethane **31** is combined with a rhodium catalyst, rapid conversion to benzophenone imine is observed (Scheme 2A). In the absence of catalyst, trace imine **32** is formed along with products of decomposition. In other contexts, we have also seen the formation of azines, which are known to arise from reaction of Rh-carbenes with diazo compounds.²⁵ Treatment of diphenyldiazomethane with a rhodium catalyst results in rapid formation of azine **34**, presumably by nucleophilic attack of the hydrazone amino group on the carbene intermediate. These two control experiments suggest that substrates prone to either slow oxidation or slow insertion may lead to undesirable by-products (Scheme 2B).



Scheme 2. A) Control reactions to determine side products of C–H insertion, B) Conditions for side product formation.

The relative rates of hydrazone oxidation and C–H insertion were studied using real-time FTIR spectroscopy. We were interested in learning how the electronic nature of the aryl ring of the hydrazone would affect the rates of both oxidation and

C–H insertion. Three hydrazones were selected for this study (eq 1). Rates of oxidation for unsubstituted **39a** and p-methoxy substituted **39b** hydrazones were similar, while the cyano substituted hydrazone (**39c**) was slower (Figure 4A). After the rhodium catalyst was added, C–H insertion proceeded rapidly in all cases (<10 minutes), as inferred from the disappearance of the diazo signal. We observe only slight differences in the rate of C–H insertion as a function of the aryl substituent. The variability in rates of oxidation based on the electronic nature of the hydrazone paired with the rapid and near constant rate of carbene formation and subsequent C–H insertion account for varying levels of imine formation from different substrates. Although the relative rates were not examined with different catalysts, it can be inferred that faster or slower catalytic rates would also have an impact on the imine formation pathway.

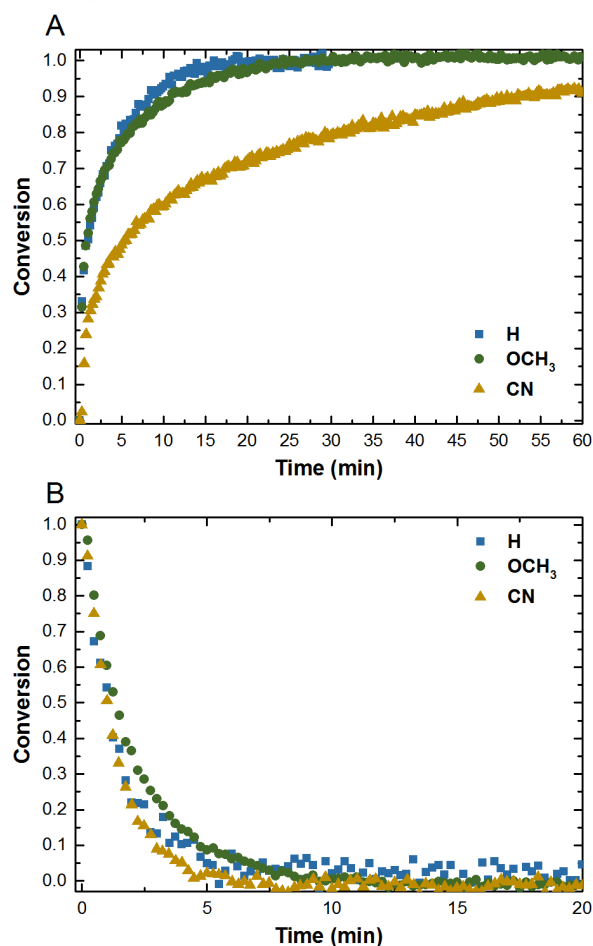
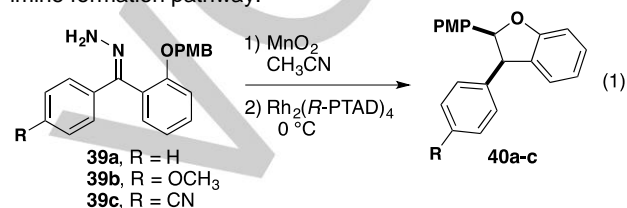


Figure 4. Reaction progress curves of conversion vs. time of (A) hydrazone oxidation and (B) C–H insertion as determined by ReactIR monitoring. The hydrazone oxidations were carried out with 8 equiv of MnO_2 in CH_3CN at 0.1 M in **39a-c** at 25 °C.

FULL PAPER

WILEY-VCH

Computational studies are consistent with the hypothesis that imine is formed by the reaction of the hydrazone with a rhodium carbene intermediate. The process was modeled at the B3LYP/6-31G(d) [C,H,N,O], LANL2DZ [Rh] level of theory²⁶, using Rh(HCO₂)₄ as a model catalyst. Addition of the hydrazone to the rhodium carbene complex is predicted to be endothermic by 3.1 kcal/mol, but proton transfer to form the precursor to fragmentation is predicted to be exothermic by 3.6 kcal/mol. The free energy barrier to fragmentation, via the transition state structure shown in Figure 5, is predicted to be only 4.1 kcal/mol (3.5 kcal/mol from separate hydrazone and carbene). The results of these calculations suggest that the process shown is indeed facile and a reasonable mechanism for imine formation is shown in Scheme 3.

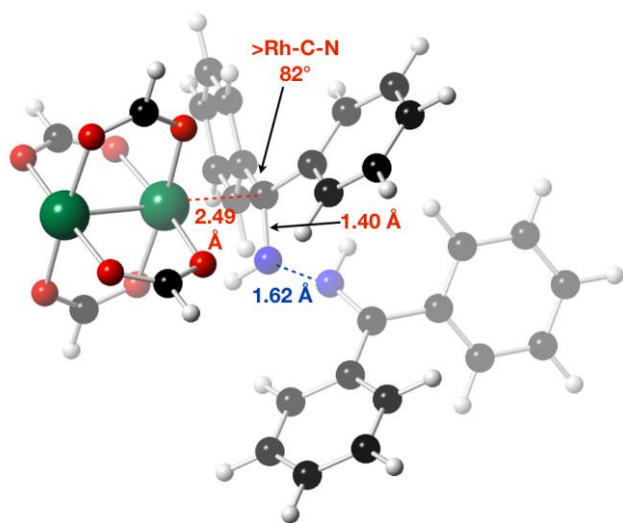
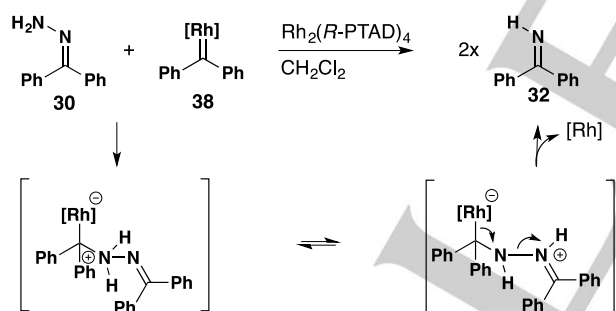


Figure 5. Fragmentation transition state structure for the formation of 32 from 30. Selected distances in Å.



Scheme 3. Proposed mechanism of imine formation.

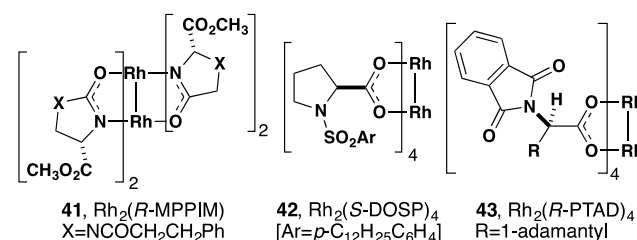
Together, these results provide a mechanistic basis for the variable reactivity that is observed in the case of the PMB ether and in other substrate classes discussed later. If both the imine oxidation and the C–H insertion are slow, then under “one-pot” conditions where all reagents are added at once, the remaining hydrazone can consume carbene intermediate to form imine, thus decreasing the yield of insertion product. This unproductive pathway can be suppressed by filtering away the MnO₂ prior to addition of the catalyst (“two-pot” conditions shown in Table 1, entry 5), or by simply allowing full conversion of the hydrazone to the diazo intermediate before treating with catalyst, i.e., the presence or absence of MnO₂ is irrelevant. If the oxidation is fast but the

C–H insertion is slow, then the diazo intermediate can dimerize to azine. Although this pathway is rarely seen for intramolecular processes, we have observed azine formation when we have attempted intermolecular reactions (not shown).

After exploring achiral catalysts, we turned our attention to controlling enantioselectivity with the hope of improving diastereoselectivity at the same time. The oxazolidinone catalyst Rh₂(4S-MPPIM)₄ **41** resulted in no observable conversion to the C–H insertion product **12** (Table 2, entry 1). Rh₂(*R*-DOSP)₄ gave rapid conversion to the desired product with a high level of diastereoselectivity (94:6) and modest enantioselectivity (36:64) (Table 2, entry 2). Finally, use of the phthalimide catalyst Rh₂(*R*-PTAD)₄ **43** produced benzodihydrofuran **12** with excellent yield, enantioselectivity and diastereoselectivity. Although reasonable effort is made to exclude water from these reactions by the use of oven-dried glassware and anhydrous solvent, the presence of water does not have a significant impact on the reaction selectivity and only slightly reduced yield is observed (Table 2, entry 6). Similar results are observed when the reaction is conducted in alcoholic solvents. These results are consistent with the greatly reduced electrophilicity of donor/donor carbene (when compared to those appended with an electron-withdrawing group), which slows down nucleophilic attack by oxygen nucleophiles such as water.

Table 2. Chiral catalysts for C–H insertion of benzyl ether 11.

entry	catalyst	solvent (temp)	dr	er	yield
1	Rh ₂ (4S-MPPIM) ₄	CH ₂ Cl ₂ (0° to rt)	-	-	-
2	Rh ₂ (<i>R</i> -DOSP) ₄	CH ₂ Cl ₂ (0° to rt)	94:6	36:64	95%
3	Rh₂(<i>R</i>-PTAD)₄	CH₂Cl₂ (0° to rt)	99:1	99:1	90%
4	Rh ₂ (<i>R</i> -PTAD) ₄	CH ₃ OH (rt)	>95:5	98:2	86%
5	Rh ₂ (<i>R</i> -PTAD) ₄	<i>i</i> -PrOH (rt)	>95:5	>99:1	76%
6	Rh ₂ (<i>R</i> -PTAD) ₄	Wet CH ₃ CN (rt)	>95:5	96:4	71%



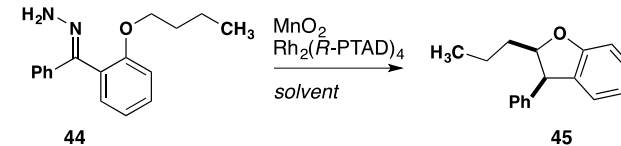
Although the reaction with Rh₂(PTAD)₄ worked with exceptional selectivity with the PMB ether in CH₂Cl₂, this was not the case as we started to explore other substrate classes. When we subjected *n*-butyl ether **44** to our one-pot conditions in CH₂Cl₂, we observed that enantioselectivity was high, yet there was no diastereoselectivity (Table 3, entry 1). When coupled with the poor yield, this provided us with an ideal substrate for solvent optimization. Nonpolar solvents pentane and toluene did little to improve this ratio (entries 2-3). Polar solvents THF and ethyl acetate provided significant boosts to the dr (entries 4-5). Finally, acetonitrile was found to be superior (entry 6) by offering the highest dr while also

FULL PAPER

WILEY-VCH

doubling the yield and only slightly compromising the er. In contrast, polar solvents are seldom used for the reactions of acceptor-substituted carbenes.²⁷ One caveat is that the solubility of $\text{Rh}_2(\text{PTAD})_4$ in acetonitrile is relatively low, which puts an upper limit on the catalyst loading. Based on the results of this screen, we opted to run the bulk of our substrate scope studies in acetonitrile.

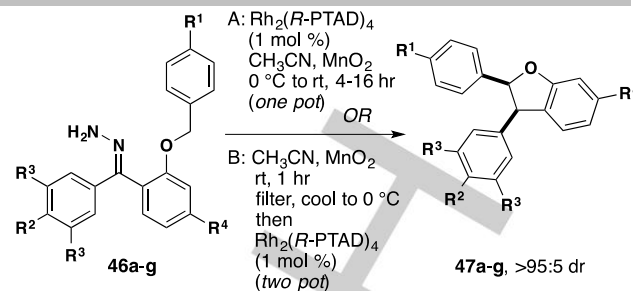
Table 3. Optimization of solvent.



entry	solvent	dr	er	yield
1	CH_2Cl_2	50:50	99:1	29%
2	toluene	55:45	-	-
3	pentane	47:53	-	-
4	EtOAc	71:29	-	-
5	THF	75:25	-	-
6	CH_3CN	81:19	94:6	58%

C–H Insertion of Benzyl Ethers. With our catalyst, solvent, and procedure set, we proceeded to examine substrate scope. Given our interest in resveratrol-derived natural products containing phenyl-substituted benzodihydrofurans, we were particularly interested in benzyl ether substrates. We were pleased to observe that $\text{Rh}_2(\text{R-PTAD})_4$ was useful for the C–H insertion of a variety of substituted benzyl ethers (Table 4). Products were isolated as a single diastereomer by NMR in each case, and enantioselectivities were excellent and appear to be unaffected by the presence of strong electron-donating or electron-withdrawing groups on any of the three aryl rings. A strong withdrawing group adjacent to the benzylic insertion site causes a reduction in yield (entries 2 and 4), but the same substitution on the pendant aryl ring has no effect (entry 9). The bulk of the substrates worked well when exposed to our one-pot conditions A, but some experienced a boost in yield, er and/or dr when exposed to our two-pot conditions B. Overall, the reaction of benzylic ethers is robust and amenable to varying electronic environments and functional groups.

Table 4. Enantioselective C–H insertion reactions of substituted benzyl ethers.

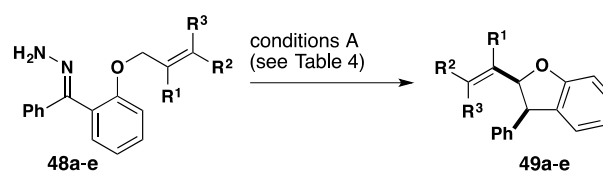


entry	product	R ¹	R ²	R ³	R ⁴	yield, er (conditions)
1	47a	Br	H	H	H	90%, 98:2 (A)
2	47b	CN	H	H	H	77%, 94:6 (A)
3 ^a	47c	NHBoc	H	H	H	89%, 2:98 (A)
4	47d	NO_2	H	H	H	63%, 98:2 (A)
5	47e	H	H	H	H	92%, 96:4 (A)
6	47f	CH_3O	H	CH_3O	H	68%, 93:7 (A)
7	47g	CH_3O	H	H	PMBO	70%, >98:2 (B)
8	47h	CH_3O	CH_3O	H	H	83%, 97:3 (B)
9	47i	CH_3O	CN	H	H	97%, 98:2 (B)

^aRun with *S*-PTAD

C–H Insertion of Allyl Ethers. Allylic ethers are attractive substrates, given their ease of synthesis and flexibility with regard to subsequent functionalization. For this substrate category, we were interested in the effects of substitution on the insertion reaction, and also the product outcome. Although a rhodium carbene with a pendant allylic ether can, in theory, undergo either C–H insertion or cyclopropanation, we only observe insertion with most substrates (Table 5). Yields are generally very high, although lack of alkene substitution and substitution close to the insertion site appear to lead to a decrease (entries 1 and 2). Enantio- and diastereoselectivities are high in all cases. Also, *E/Z* isomerization is not observed (entries 3 and 4). These substrates were all run with conditions A - our “one-pot” method.

Table 5. Enantioselective C–H insertion reactions of substituted allyl ethers.



entry	product	R ¹	R ²	R ³	dr	er	yield
1	49a	H	H	H	97:3	93:7	77% ^a
2	49b	CH_3	H	H	92:8	97:3	70%
3	49c	H	H	<i>n</i> -Pr	98:2	98:2	95% ^b
4	49d	H	<i>n</i> -Pr	H	94:6	93:7	92% ^c
5	49e	H	CH_3	CH_3	>95:5	97:3	96%

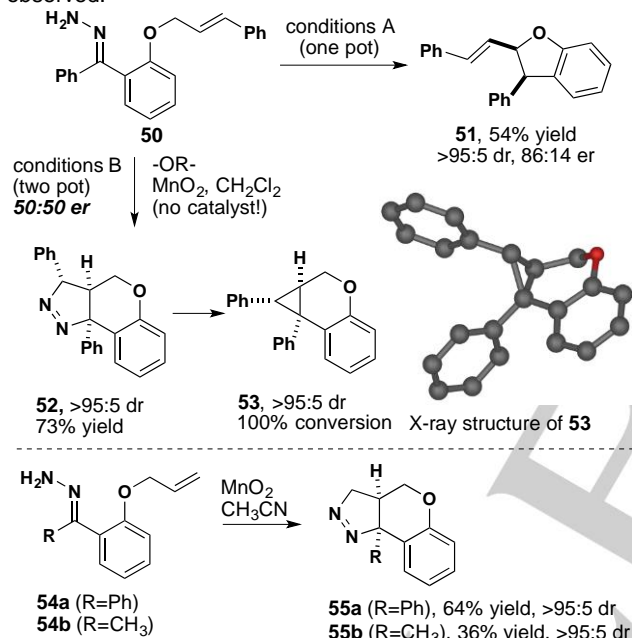
^aRun in CH_2Cl_2 ; ^b>95:5 *Z*; ^c>95:5 *E*

Attempted insertion reactions of cinnamyl ether **50** revealed an alternate, non-catalytic reaction pathway. When insertion of **50** was first attempted with conditions A, formation of the expected benzodihydrofuran **51** was observed with modest yield and enantioselectivity (Scheme 4). When conditions B were used in an attempt to boost yield and selectivity, rapid conversion to fused pyrazoline **52** by an intramolecular dipolar cycloaddition (DPC) was observed. Following this

FULL PAPER

WILEY-VCH

result, the hydrazone was subjected to MnO_2 with no catalyst present, also resulting in the DPC product. DPC reactions of diazo compounds with alkenes are well-documented²⁸ and a recent report from the Zard group provides close precedent for our results²⁹. Full characterization of **52** proved to be elusive due to its rapid thermal nitrogen extrusion³⁰, resulting in cyclopropane product **53**, whose structure was determined unambiguously by X-ray crystallography. Chemical shift and splitting values from a full set of 2-D NMR spectroscopy (COSY, HSQC, HMBC, NOESY, TOCSY, ^1H - ^{15}N HSQC) were consistent with NMR chemical shifts and coupling constants computed with density functional theory (DFT)³¹. Two additional allylic ethers were cyclized to produce pyrrazoles **55a** and **55b**. The cyclization product **54b** was formed previously with a similar method by Zard, and the spectral data is consistent with theirs²⁹. Given three potential pathways of reactivity, these results demonstrate that rhodium-catalyzed C–H insertion outpaces intramolecular DPC in most cases, and direct cyclopropanation is never observed.



Scheme 4. Competing insertion and uncatalyzed 1,3-dipolar cycloaddition pathways for cinnamyl ether **50**.

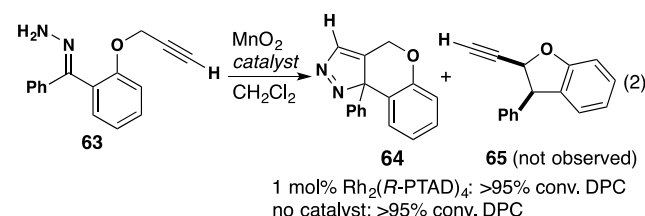
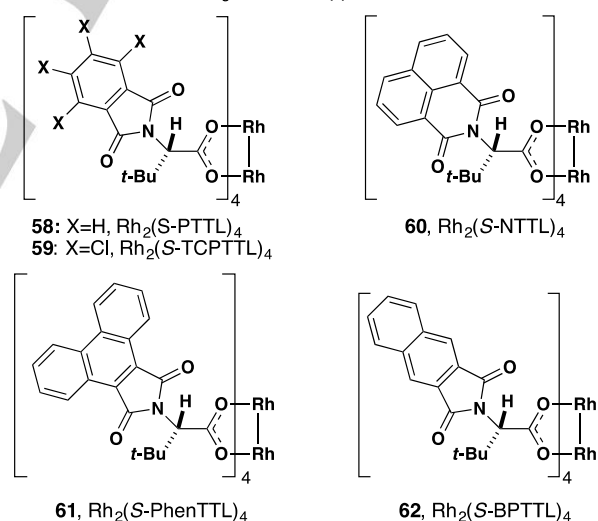
C–H Insertion of Propargyl Ethers. Alkyne substitution on the C–H insertion substrate presented an opportunity for catalyst optimization. Phenylpropargyl ether **56** underwent substitution with high diastereoselectivity and yield, yet the enantiomer ratio was among the lowest observed (Table 6, entry 1). Although the er was improved greatly by running the reaction in CH_2Cl_2 , the yield was halved (entry 2). Additional PTAD-like catalysts were tested in the hope of improving these two areas. $\text{Rh}_2(\text{S-PTTL})_4$ (**58**), $\text{Rh}_2(\text{S-TCPTTL})_4$ (**59**), and $\text{Rh}_2(\text{S-BPTTL})_4$ (entries 3, 4, and 7) afforded roughly the same yield and lower enantioselectivities than $\text{Rh}_2(\text{S-PTAD})_4$. A large increase in yield was noted for $\text{Rh}_2(\text{S-NTTL})_4$ (**60**) and $\text{Rh}_2(\text{S-PhenTTL})_4$ (**61**) (entries 5 and 6), however the enantioselectivity was diminished in both cases.

The attempted insertion of unsubstituted propargyl ether **63** led primarily to the DPC product. Hydrazone **63** was subjected to our standard one-pot conditions with $\text{Rh}_2(\text{R-PTAD})_4$ in CH_2Cl_2 . The major product was pyrazole **64** from 1,3-dipolar cycloaddition, in analogy to the competing pathway for allylic substrates (eq 2). Some signals in the ^1H NMR spectrum of the unpurified reaction mixture suggest that insertion product **65** was formed in small quantities. Stirring hydrazone **63** with only MnO_2 afforded the DPC product as the sole product. Phenyl substitution of an alkene accelerated the formation of DPC. In contrast, phenyl substitution of the analogous alkyne caused a reduction in rate of DPC formation, potentially due to increased sterics and less flexibility in the substrate.

Table 6. Enantioselective C–H insertion reactions of propargyl ether **56**.

entry	catalyst	er	yield
1 ^a	R-PTAD ^b	68:32	76%
2	S-PTAD	20:80	34%
3	58	23:77	38%
4	59	29:71	39%
5	60	42:58	81%
6	61	31:69	64%
7	62	35:65	34%

^aReaction was run in CH_3CN , ^bThe opposite enantiomer was obtained



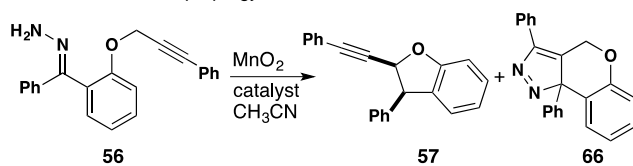
When phenyl substituted alkyne **56** was revisited, it was revealed that the DPC product is formed to varying degrees. With $\text{Rh}_2(\text{PTAD})_4$ as the catalyst, the major product is C–H insertion (Table 7, entry 1), highlighting the high reactivity of this catalyst. With $\text{Rh}_2(\text{OAc})_4$, dipolar cycloaddition is the major pathway (entry 2). Although reduced temperature shifts

FULL PAPER

WILEY-VCH

the reaction toward C–H insertion, cycloaddition is still the dominant pathway. As with **63**, omission of the catalyst yields the DPC product **66** in high yield.

Table 7. Reactions of propargyl ether **56**.

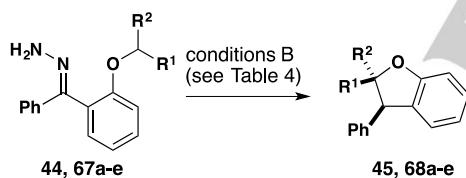


entry	catalyst	temperature (°C)	ratio (57 : 66)	yield
1	$\text{Rh}_2(\text{R-PTAD})_4$	0	89:11	76% (57)
2	$\text{Rh}_2(\text{OAc})_4$	rt	6:94	78% (66)
3 ^a	$\text{Rh}_2(\text{OAc})_4$	-20	40:60	-
4	none	rt	0:100	81% (66)

^aReaction was run in CH_2Cl_2

C–H Insertion of Alkyl Ethers. Alkyl ethers were challenging substrates that demonstrated the limits of this methodology. Although conditions B worked well for several branched ethers, the er was slightly diminished in the case of isopropyl ether **67d** (Table 8). Methyl ether **67e** proceeded with poor conversion and modest er. The yield could be improved with a shorter oxidation time (entry 6). The low reactivity is expected, because hydride transfer is believed to be the first event in a concerted, asynchronous reaction that is followed by rapid collapse of the metal-bound anion and pendant cation³². The poor enantioselectivity is not surprising due to the low steric demand of the methyl ether, especially when viewed in comparison to our computational results for more substituted reactants (see below).

Table 8. C–H insertion reactions of alkyl ethers.



entry	product	R ¹	R ²	dr	er	yield
1	45	<i>n</i> -Pr	H	89:11	97:3	79%
2	68b	<i>i</i> -Pr	H	89:11	97:3	88%
3	68c	<i>i</i> -Bu	H	88:12	94:6	81%
4	68d	CH_3	CH_3	-	81:19	76%
5 ^a	68e	H	H	-	35:65	20%
6 ^b	68e	H	H	-	22:78	49%

^aReaction was run with $\text{Rh}_2(\text{S-PTAD})_4$ in CH_2Cl_2

^bHydrazone was converted to diazo compound with MnO_2 at room temperature before the mixture was cooled to 0 °C and $\text{Rh}_2(\text{R-PTAD})_4$ added.

Origin of Stereoselectivity. Computation was used to query the mechanism of the intramolecular C–H insertion reaction to form dihydrobenzofuran products. A concerted mechanism for reactions of Rh-carbenes has been proposed based on DFT calculations by Nakamura and co-workers³². A concerted mechanism had also been proposed for intramolecular C–H insertion reactions by Taber and co-workers based on semi-empirical calculations³³. Taber's model proved very effective for predicting stereochemical

outcomes of C–H insertion events. Based on DFT calculations, intermolecular cyclopropanation reactions have also been proposed to follow a concerted pathway³⁴. However, our more recent experimental studies on intramolecular cyclopropanation reactions to form bicyclobutanes led us to propose a stepwise mechanism involving an ylide intermediate³⁵. Similarly, we considered that a zwitterionic pathway might also prove relevant to intramolecular C–H insertion reactions, where geometric constraints would render difficult a mechanism involving concerted C–H insertion.

A mechanistic model for the intramolecular C–H insertion reaction was developed computationally as shown in Figure 6. For carbene **69**, a transition state structure (**TS1**) was located for *hydride transfer* to give ylide intermediate **70**. This same transition state structure was observed from several starting geometries, including one where the C–H bond and the $\text{Rh}=\text{C}$ were aligned as in Nakamura's transition state for concerted C–H insertion³². With a very low barrier ($\Delta H^\ddagger = 4.0$ kcal/mol with M06-2X/LANL2DZ [6-311+G(d,p)]; 2.4 kcal/mol with B3LYP/LANL2DZ[6-31G(d)]), ylide **70** proceeds to the formal C–H insertion product via a second transition state structure (**TS2**). The predicted barrier for the highly exothermic conversion of ylide **70** into product **12** is much lower than the expected barrier for isomerization of the oxonium of intermediate **70**.³⁶ Because **TS2** represents the barrier to a stereospecific process, the diastereoselectivity should be governed by **TS1**. Moreover, this very low barrier is consistent with many previous examples in which C–H insertion at stereocenters has been shown to be stereospecific, as the conversion of ylide **70** into product **12** is expected to be fast and hence stereospecific.

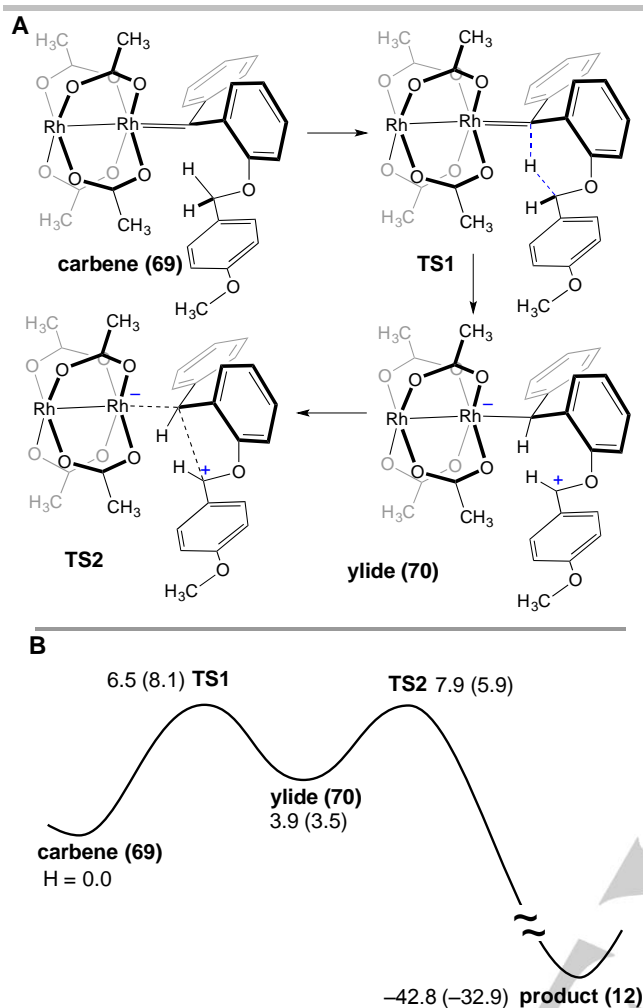
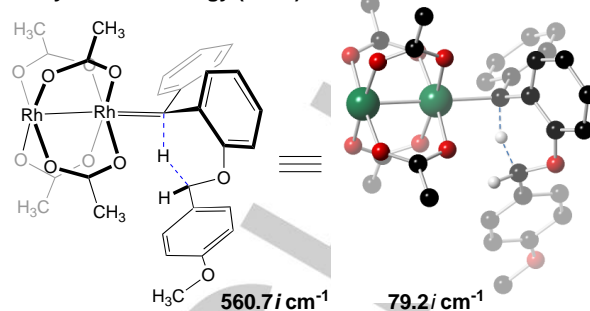


Figure 6. (A) Proposed mechanism for C–H insertion involving an ylide intermediate (**70**) that proceeds to dihydrobenzofuran product with a very low barrier (**TS2**). (B) Enthalpy vs reaction coordinate for the conversion of carbene **69** into product **12** via ylide **70**. Enthalpies are in kcal/mol. Energies at the M06-2X/LANL2DZ [6-311+G(d,p)] level are shown first, with enthalpies at the B3LYP/LANL2DZ[6-31G(d)] level in parentheses.

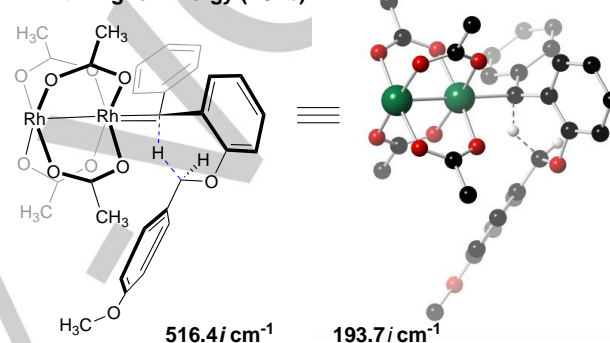
Computation was also used to probe the diastereoselectivity for the transformation of carbene **69** into ylide **70**. As shown in Figure 7, two transition state structures were located—**TS1a**, which leads to the syn-diastereomer, and **TS1b**, which leads to the anti-diastereomer. For **TS1b**, the enthalpic barrier was 1.4 kcal/mol higher at the M06-2X/LANL2DZ [6-311+G(d,p)] level, and 2.0 kcal/mol higher at the B3LYP/LANL2DZ[6-31G(d)] level. Similar differences between the two transition states were observed when ΔE^\ddagger , $\Delta E(\text{ZPE})^\ddagger$ and ΔG^\ddagger were compared (Supporting Information). These computational findings are consistent with the experimental finding that the syn-diastereomer is favored.

A. Syn: Lower Energy (TS1a)



m062x/LANL2DZ [6-311+G(d,p)]: DH^\ddagger 6.5 kcal/mol
B3LYP/LANL2DZ[6-31G(d)]: DH^\ddagger 8.1 kcal/mol

B. Anti: Higher Energy (TS1b)



m062x/LANL2DZ [6-311+G(d,p)]: DH^\ddagger 7.9 kcal/mol
B3LYP/LANL2DZ[6-31G(d)]: DH^\ddagger 10.1 kcal/mol

Figure 7. Transition state structures for initial hydride transfer step leading to (A) syn- and (B) anti-diastereomers.

The $\text{Rh}_2(\text{OAc})_4$ -derived transition state structures were used to develop a model to rationalize the high levels of enantioselectivity and diastereoselectivity observed with $\text{Rh}_2(\text{S-PTAD})_4$ catalyzed C–H insertion reactions. This model assumes that $\text{Rh}_2(\text{S-PTAD})_4$ adopts a ‘chiral crown’ structure,³⁷ similar to that observed for $\text{Rh}_2(\text{S-PTTL})_4$, where all of the phthalimido groups are projected on the same face of the catalyst (the chiral crown structure has recently been observed in a $\text{Rh}_2(\text{S-PTTL})_4[\text{C}(\text{Ar})\text{COOMe}]$).³⁸ Starting with the known structure of $\text{Rh}_2(\text{S-PTTL})_4$ ³⁹ and the core structure of $\text{Rh}_2(\text{OAc})_4$ -derived transition state structure **TS1a**, we were able to locate the transition state structure shown in Figure 8. Calculations were carried out at the B3LYP/LANL2DZ[6-31G(d)] level. In this transition state structure, which leads to **syn-(R)-12**, the chiral crown structure of the catalyst is maintained without incurring any offensive steric interactions. An attractive C–H π interaction⁴⁰ (2.82 Å) between the substrate-derived phenyl group and a ligand phthalimido was observed. We also located transition state structures that would lead to the diastereomeric product **anti-(S)-12** as well as the enantiomeric product **syn-(S)-12**, which were higher in energy by 4.7 and 6.1 kcal/mol, respectively, relative to the transition state structure leading to **syn-(R)-12** (Supporting Information). These transition state structures both incurred significant interactions between substrate and ligand fragments. While the large size and conformational flexibility of these complexes makes a complete comprehensive analysis nearly impossible, we were

FULL PAPER

WILEY-VCH

not able to locate alternate transition state structures that maintain the chiral crown structure of $\text{Rh}_2(\text{S-PTTL})_4$ without incurring such steric interactions.

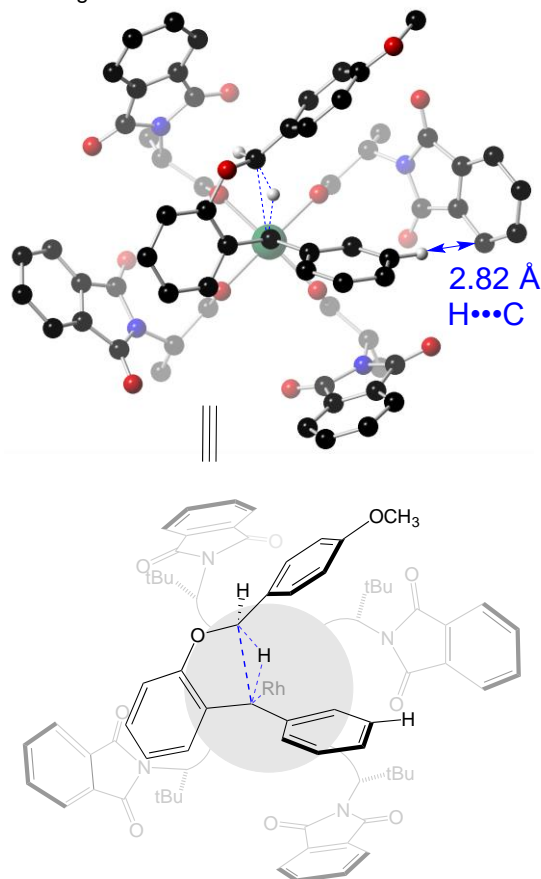


Figure 8. Transition state for the initial hydride transfer step in the reaction leading to *syn*-(*R*)-12. The carbene is derived from $\text{Rh}_2(\text{S-PTTL})_4$, a structurally similar analog to $\text{Rh}_2(\text{S-PTAD})_4$ with *t*-Bu groups instead of adamantyl groups. The *t*-Bu groups are not shown for clarity. Calculations were carried out at the B3LYP/LANL2DZ[6-31G(d)] level.

Conclusions

In summary, we have developed the C–H insertion reaction of donor/donor diaryl rhodium carbenes for the enantioselective synthesis of benzodihydrofurans. Our method enables the rapid assembly of enantioenriched benzodihydrofuran cores in one step from diaryl hydrazones. The reaction is robust and amenable to the presence of water, varying functional groups and steric factors. Computation has led to a robust mechanistic model and provides an explanation for the high enantio- and diastereoselectivity observed. Several side pathways have been thoroughly investigated and characterized. This synthetic method should be valuable in the future synthesis of natural products and other compounds with a benzodihydrofuran core.

Experimental Section

Materials and Instrumentation:

Unless otherwise specified, all commercially available reagents were used as received. All reactions using dried solvents were carried out

under an atmosphere of argon in oven-dried glassware with magnetic stirring. Dry solvent was dispensed from a solvent purification system that passes solvent through two columns of dry neutral alumina. ^1H NMR spectra and proton-decoupled ^{13}C NMR spectra were obtained on a 400 MHz Bruker or a 600 MHz Varian NMR spectrometer. Chemical shifts (δ) are reported in parts per million (ppm) relative to TMS (s, δ 0). Multiplicities are given as: s (singlet), d (doublet), t (triplet), q (quartet), p (pentet), h (hexet), and m (multiplet). Complex splitting will be described by a combination of these abbreviations, i.e. dd (doublet of doublets). ^{13}C NMR chemical shifts are reported relative to CDCl_3 (t, δ 77.4) unless otherwise noted. High-resolution mass spectra were recorded on positive ESI mode unless otherwise noted. Melting points were taken on an EZ-melting apparatus and were uncorrected. Infrared spectra were taken on a Bruker Tensor 27 spectrometer. Chromatographic purifications were performed by flash chromatography with silica gel (Fisher, 40–63 μm) packed in glass columns. The eluting solvent for the purification of each compound was determined by thin-layer chromatography (TLC) on glass plates coated with silica gel 60 F254 and visualized by ultraviolet light. Abbreviations for frequently used chemicals will be seen as follows: dichloromethane (CH_2Cl_2), ethanol (EtOH), ethyl acetate (EtOAc), methanol (CH_3OH), tetrahydrofuran (THF), acetonitrile (CH_3CN). Diastereoselectivity of the C–H insertion reactions was measured primarily by crude ^1H NMR (compounds listed as >95:5), with some substrates measured by GC-MS (compounds listed as >99:1). In situ FT-IR monitoring was conducted with a Mettler-Toledo ReactIR 15 equipped with a DiComp (Diamond) ATR probe connected via an AgX (silver halide) 6 mm x 1.5 m fiber optic cable. Reaction temperatures were monitored using an internal thermistor in the IR probe. Sampling was carried out over 2000–800 cm^{-1} at 4 wavenumber resolution with 1x gain. The formation and consumption of the diazo intermediate was performed by tracking the IR peak height at 1316 or 1280 cm^{-1} over time relative to a signal point baseline.

General Procedure A for the Synthesis of Benzophenones:

In a flame-dried flask, 2-hydroxybenzophenone (0.5 g, 2.5 mmol) and anhydrous Cs_2CO_3 (2.44 g, 7.5 mmol) were dissolved in anhydrous acetonitrile (25 mL, 0.1 M). The desired alkyl bromide (3 mmol) was added slowly, and the reaction was heated at 50 $^\circ\text{C}$ for 3–18 hours. Following completion (determined by TLC), the Cs_2CO_3 was removed via filtration, then the solvent was removed in vacuo to give the crude product. Purification using column chromatography with 10–20% EtOAc/hexanes as the eluent afforded the desired alkylated product.

General Procedure B for the Synthesis of Benzophenones:

To a flask was added 2-hydroxybenzophenone (0.5 g, 2.5 mmol), the desired alcohol (2.5 mmol) along with anhydrous THF (25 mL, 0.1 M). After cooling to 0 $^\circ\text{C}$, PPh_3 (0.787 g, 3 mmol) and diisopropyl azodicarboxylate (DIPAD) (0.589 mL, 3 mmol) were added and the reaction was stirred overnight while coming to room temperature. The solvent was evaporated, and careful purification using column chromatography with 5–10% EtOAc/hexanes as the eluent afforded the desired alkylated product.

General Procedure C for the Synthesis of Dibenzyl Alcohols:

In a flame-dried flask purged with argon, aryl bromide (1 equiv.) was dissolved in THF (0.24M) and cooled to -78 $^\circ\text{C}$. Butyllithium solution (1.1 equiv., 2.5 M in hexanes) was added dropwise, and the reaction was stirred at -78 $^\circ\text{C}$ for 20–40 minutes. The desired aldehyde (1.05 equiv., 0.37 M in THF) was then added dropwise, and the reaction was stirred for an hour before it was allowed to warm slowly to room temperature over an additional three to four hours. The reaction was quenched with a volume of saturated ammonium chloride solution equal to the volume of aryl bromide solution and diluted with an equivalent amount of water. The aqueous layer was extracted three

times with EtOAc, and the combined organic layers were washed one time each with water and brine. The organic layer was then dried over Na₂SO₄, filtered and concentrated *in vacuo* to afford the crude product. Purification using column chromatography with 20-30% EtOAc/hexane solution provided the desired product.

General Procedure D for the Synthesis of Benzophenones:

To a flame-dried flask purged with argon was added the alcohol from General Procedure D (1.0 equiv), solid NaHCO₃ (10 equiv.) and dry CH₂Cl₂ (0.13M). Dess-Martin periodinane (1 equiv.) was added and the reaction was stirred at room temperature for 2-4 hours. The reaction was quenched with a volume of saturated Na₂SO₃ equal to half the volume of CH₂Cl₂ and was stirred for 5 minutes. An equal volume of saturated NaHCO₃ solution was then added, and the aqueous layer was extracted with EtOAc three times. The combined organic layers were washed one time each with water and brine, then dried over Na₂SO₄, filtered and concentrated *in vacuo* to afford the desired ketone product. This product was carried forward without further purification. The ketone (1 equiv.) was taken up in dry CH₂Cl₂ (0.1M) and cooled to 0 °C. BCl₃ (1.5 equiv., 1.0 M in CH₂Cl₂) was added dropwise, and the reaction was stirred at 0 °C for one hour. The reaction was quenched with a volume of saturated ammonium chloride equal to the volume of CH₂Cl₂. The aqueous layer was extracted three times with CH₂Cl₂, and then the combined organics were washed one time each with water and brine. The organic layer was dried over Na₂SO₄, filtered and concentrated to afford crude product. This product was taken immediately into the next reaction without further purification. The phenol (1 equiv.) was dissolved in acetonitrile (0.1M) under argon. To the flask was added Cs₂CO₃ (3 equiv.) and PMBCl (1.2 equiv.) and the reaction was heated at 50 °C overnight. The Cs₂CO₃ was filtered off, and the filtrate was concentrated *in vacuo* to afford crude product. Purification using column chromatography with 20-30% EtOAc/hexane solution afforded the desired product.

General Procedure E for the Synthesis of Hydrazones:

To a flame-dried flask was added anhydrous EtOH (0.06 M) along with the desired alkylated benzophenone (1 equiv.) from General Procedure A, B, or D. Glacial acetic acid (1.2 equiv) was added followed by anhydrous hydrazine (6 equiv.), and the reaction was heated to 80 °C overnight. After the EtOH was removed *in vacuo*, the residue was taken up in Et₂O and water. The layers were separated and the organic layer was washed with water (2 x 20 mL). The combined organic layers were dried using anhydrous sodium sulfate, filtered, and concentrated *in vacuo*. The crude material was purified using column chromatography (15-25% EtOAc/hexanes) to afford the desired product. Yields were typically seen between 60-90%.

General Procedure F for the screening of achiral catalysts:

To a vial was added hydrazone **11** (25.0 mg, 0.075 mmol) and the desired rhodium catalyst (7.5 X 10⁻⁴ mmol, 1 mol%). The vial was flushed with Ar and CH₂Cl₂ (4.7 mL, 0.016M) was added. MnO₂ (52.1 mg, 0.6 mmol) was added last, and the vial was capped and covered with foil. The reaction was run overnight at room temperature, filtered through celite and concentrated to afford the crude product. Diastereoselectivity and product ratios were assessed by ¹H NMR. The residue was purified by flash column chromatography (10:90 EtOAc/hexanes) to provide insertion product.

General Considerations for the Synthesis of Novel Achiral Catalysts:

All reactions were carried out in glassware that was flame-dried under vacuum and cooled under nitrogen. Dichloromethane, toluene and hexanes were dried with columns packed with activated neutral

alumina. Tetrahydrofuran was freshly distilled from sodium/benzophenone. Anhydrous chlorobenzene was purchased from Acros. Rh₂(OAc)₄ was purchased from Pressure Chemicals. Chromatography was performed on silica gel (Silicycle Siliacflash 40-63µm, 60Å). Reagents were used directly as purchased from commercial sources without further purification. For ¹³C NMR, multiplicities were distinguished using an ATP pulse sequence: typical quaternary and methylene carbon appears 'up' (C or CH₂); methane and methyl carbons appears 'down' (CH or CH₃). High-resolution mass spectrometry (HRMS) was performed using Liquid Injection Field Desorption Ionization (LIFDI) coupled with a time of flight (TOF) detector. Dirhodium tetrakis(tri(4-fluorophenyl)acetate (**16**),⁴¹ dirhodium tetrakisbenzoate (**19**),⁴² dirhodium tetrakis(2-(4-fluorophenyl)-2-methylpropanoate (**24**), and dirhodium tetrakis (2-methyl-2-phenyl)propanoate (**26**),⁴³ were prepared by methods in the literature.

General Procedure G for the synthesis of Tetrakis dirhodium (II) complexes:

To a flame dried round-bottomed flask equipped with a pressure equalizing addition funnel containing a plug of cotton and Na₂CO₃ (for removal of acetic acid) and a reflux condenser was charged with dirhodium tetraacetate (50 mg, 0.113 mmol, 1.0 equiv) and the appropriate carboxylic acid (1.13 mmol, 10 equiv) and the apparatus was evacuated and filled with nitrogen. Anhydrous chlorobenzene was added and the mixture was heated to reflux for 12 h. The solvent was subsequently distilled off and the green residue was dissolved in CH₂Cl₂, washed three times with aqueous saturated sodium bicarbonate, dried over anhydrous MgSO₄, filtered, concentrated, and chromatographed on silica gel to give the title compound as a green solid.

General Procedure H for the synthesis of racemic benzodihydrofurans:

The desired hydrazone (1 eq) was dissolved in acetonitrile or CH₂Cl₂ (0.016M) under argon atmosphere. The flask was wrapped in foil, then MnO₂ (8 eq.) was added followed by Rh₂(OAc)₄ (0.01 eq). The reaction was stirred from 3-18 hours at room temperature. Following reaction completion, the MnO₂ was removed by passing the crude reaction through a plug of celite or silica and rinsing several times with CH₂Cl₂. The solvent was removed *in vacuo* to give the crude product. Column chromatography using 2-5% EtOAc/hexanes as the eluent afforded the desired product.

General Procedure I for the synthesis of chiral benzodihydrofurans (Method A):

In a flame-dried flask, the desired hydrazone (1 equiv.) was dissolved in acetonitrile (0.016 M) under argon atmosphere. The flask was placed in an ice bath wrapped in foil, then MnO₂ (8 equiv.) was added followed by Rh₂(*R*-PTAD)₄ (0.01 eq). The reaction was stirred from 3-18 hours while coming to room temperature. Following reaction completion, the MnO₂ was removed by passing the crude reaction through a plug of silica or celite and rinsing several times with CH₂Cl₂. The solvent was removed *in vacuo* to give the crude product. Column chromatography using 2-5% EtOAc/hexanes as the eluent afforded the desired product.

General Procedure J for the synthesis of chiral benzodihydrofurans (Method B):

In a flame-dried flask, the desired hydrazone (1 equiv.) was dissolved in acetonitrile (0.1 M) under argon atmosphere. The flask was wrapped in foil, and MnO₂ (8 equiv.) was added. The oxidation was allowed to stir for 1 hour, then reaction was filtered through celite into a new flame-dried flask. The bright orange diazo compound was

FULL PAPER

WILEY-VCH

diluted to 0.015 M, cooled to -20 or 0 °C, and the Rh₂(R-PTAD)₄ catalyst was added. The insertion reaction was stirred for 3-18 hours. The solvent was then evaporated to give the crude product. Column chromatography using 2-5% EtOAc/hexanes afforded the desired product.

General Procedure K for the in-situ monitoring of the C–H insertion reaction

A flame-dried three-necked round bottom flask and magnetic stir bar was fitted with two rubber septa (left and right ports) and a glass stopper (center port). Through one of the side septa a hole was bored through which the IR probe was inserted. The resulting setup was cooled under argon and placed into a preheated water bath set at 25 °C. After configuring the IR acquisition parameters, acetonitrile (5 mL) was then added and the instrument was blanked. The spectral acquisition was initiated and a baseline signal was acquired. After a stable signal was achieved, hydrazone (.5 mmol, 0.1 M) was added through the center port and was allowed to stir for ~20 min to allow for thermal equilibration. MnO₂ (348 mg, 4 mmol, 8 equiv.) was then added in one portion and the resulting suspension was allowed to stir vigorously until there was no noticeable change in the diazo signals. For the cyclization, an additional 5 mL aliquot of acetonitrile was added to the stirring reaction to obtain a nominal concentration of 0.5 M. The water bath was then replaced with an ice bath. After the reaction temperature become constant (~30 min), Rh₂(R-PTAD)₄ (7.80 mg, 0.005 mmol, 0.01 equiv.) was added.

Acknowledgements

KNL acknowledges support from the Department of Education GAANN Fellowship, the Department of Chemistry Borge Fellowship, and the UC Davis Graduate Research Award. AJK thanks UC Davis Provost Undergraduate Fellowship (PUF) and the Arnold and Mabel Beckman Foundation. CS thanks CAPES (Coordenação de Aperfeiçoamento de Pessoal de Nível Superior) and the Brazilian Ministry of Education for a postdoctoral fellowship. JH gratefully acknowledge Mettler-Toledo Autochem for the donation of an EasyMax 402 Process Reaction Platform. Additionally, we thank Merck Research Labs for student research fellowships (to R.C.). MCR would like to acknowledge the Ministerio de Educación y Ciencia for the FPU fellowship and to the Fundación Pedro Barrié de la Maza for a fellowship to visit the Tantillo lab and professors Carlos Silva López and Olalla Nieto Faza for helpful comments.

Keywords: keyword 1 • keyword 2 • keyword 3 • keyword 4 • keyword 5

[1] a) Reddy, R. P.; Lee, G. H.; Davies, H. M. L. *Org. Lett.* **2006**, *8*, 3437-3440; b) Davies, H. M. L.; Bruzinski, P. R.; Lake, D. H.; Kong, N.; Fall, M. J. *J. Am. Chem. Soc.* **1996**, *118*, 6897-6907.

- [2] Doyle, M. P.; Brandes, B. D.; Kazala, A. P.; Pieters, R. J.; Jarstfer, M. B.; Watkins, L. M.; Eagle, C. T. *Tetrahedron Lett.* **1990**, *31*, 6613-6616.
- [3] For comprehensive reviews on C–H insertion, see: a) Doyle, M. P.; Duffy, R.; Ratnikov, M.; Zhou, L. *Chem. Rev.* **2010**, *110*, 704-724; b) Davies, H. M. L.; Denton, J. R. *Chem. Soc. Rev.* **2009**, *38*, 3061-3071; c) Santiago, J. V.; Machado, A. H. L. *Beilstein J. Org. Chem.* **2016**, *12*, 882-902.
- [4] a) Taber, D. F.; Petty, E. H. *J. Org. Chem.* **1982**, *47*, 4808-4809; b) Taber, D. F.; Ruckle, R. E. *J. Am. Chem. Soc.* **1986**, *108*, 7686-7693; c) Doyle, M. P.; Van Oeveren, A.; Westrum, L. J.; Protopopova, M. N.; Clayton, T. W. *J. Am. Chem. Soc.* **1991**, *113*, 8982-8984
- [5] a) Ye, T.; McKervey, M. A. *Chem. Rev.* **1994**, *94*, 1091-1160; b) Doyle, M. P.; Forbes, D. C. *Chem. Rev.* **1998**, *98*, 911-936.
- [6] a) Davies, H. M. L.; Hansen, T. J. *Am. Chem. Soc.* **1997**, *119*, 9075-9076; b) Davies, H. M. L.; Denton, J. R. *Chem. Soc. Rev.* **2009**, *38*, 3061-3071; c) Davies, H. M. L.; Pelphrey, P. M. *Organic Reactions (Hoboken, NJ, United States)* **2011**, *75*, 75-212.
- [7] a) Zhu, D.; Ma, J.; Luo, K.; Fu, H.; Zhang, L.; Zhu, S. *Angew. Chem., Int. Ed.* **2016**, *55*, 8452-8456; b) Ma, X.; Wu, F.; Yi, X.; Wang, H.; Chen, W. *Chem. Commun.* **2015**, *51*, 6862-6865; c) Zhang, Y.; Wang, D.; Cui, S. *Org. Lett.* **2015**, *17*, 2494-2497.
- [8] Examples of metal-catalyzed reactions of diaryldiazomethanes include: a) Mehrotra, K. N.; Singh, G. S. *Indian J. Chem., Sect. B: Org. Chem. Incl. Med. Chem.* **1985**, *24B*, 773-774. b) Werner, H.; Schneider, M. E.; Bosch, M.; Wolf, J.; Teuben, J. H.; Meetsma, A.; Troyanov, S. I. *Chem. Eur. J.* **2000**, *6*, 3052-3059. e) Petursson, S. *Carbohydr. Res.* **2001**, *331*, 239-245. f) Petursson, S.; Jonsdottir, S. *Tetrahedron Asymmetry* **2012**, *23*, 157-163; g) Qiu, L.; Huang, D.; Xu, G.; Dai, Z.; Sun, J. *Org. Lett.* **2015**, *17*, 1810-1813; h) Zhang, Y.; Wang, D.; Cui, S. *Org. Lett.* **2015**, *17*, 2494-2497.
- [9] a) Ma, X. J.; Wu, F. F.; Yi, X. F.; Wang, H. X.; Chen, W. Z. *Chem. Comm.* **2015**, *51*, 6862-6865; b) Zhu, D.; Ma, J.; Luo, K.; Fu, H. G.; Zhang, L.; Zhu, S. F. *Angew. Chem. Int. Ed.* **2016**, *55*, 8452-8456. c) W. H. Cheung, S. L. Zheng, W. Y. Yu, G. C. Zhou, C. M. Che, *Org. Lett.* **2003**, *5*, 2535-2538; d) X. L. Dai, T. H. Warren, *J. Am. Chem. Soc.* **2004**, *126*, 10085-10094. e) M. P. Doyle, K. G. High, S. M. Oon, A. K. Osborn, *Tetrahedron Lett.* **1989**, *30*, 3049-3052; f) M. A. Garcia-Garibay, H. Dang, *Org. Biomol. Chem.* **2009**, *7*, 1106-1114; g) Y. Li, J. S. Huang, Z. Y. Zhou, C. M. Che, X. Z. You, *J. Am. Chem. Soc.* **2002**, *124*, 13185-13193; h) H. Werner, M. E. Schneider, M. Bosch, J. Wolf, J. H. Teuben, A. Meetsma, S. I. Troyanov, *Chem. Eur. J.* **2000**, *6*, 3052-3059; i) S. L. Zheng, W. Y. Yu, M. X. Xu, C. M. Che, *Tetrahedron Lett.* **2003**, *44*, 1445-1447.
- [10] Soldi, C.; Lamb, K. N.; Squitieri, R. A.; González-López, M.; Di Maso, M. J.; Shaw, J. T. *J. Am. Chem. Soc.* **2014**, *136*, 15142-15145.
- [11] a) Werlé, C.; Goddard, R.; Fürstner, A. *Angew. Chem., Int. Ed.* **2015**, *54*, 15452-15456; b) Werlé, C.; Goddard, R.; Philipps, P.; Farès, C.; Fürstner, A. *J. Am. Chem. Soc.* **2016**, *138*, 3797-3805
- [12] Sun, X. X.; Zhang, H. H.; Li, G. H.; Meng, L.; Shi, F. *Chem. Commun.* **2016**, *52*, 2968-2971.
- [13] Resveratrol in Health and Disease; Aggarwal, B. B., Shishodia, S., Eds.; CRC Press, Taylor and Francis Group: Boca Raton, FL, 2006.
- [14] Pezet, R.; Perret, C.; Jean-Denis, J. B.; Tabacchi, R.; Gindro, K.; Viret, O. *J. Agric. Food. Chem.* **2003**, *51*, 5488-5492.
- [15] Sato, M.; Tsuchiya, H.; Miyazaki, T.; Ohyama, M.; Tanaka, T.; Iinuma, M. *Lett. Appl. Microbiol.* **1995**, *21*, 219-222.
- [16] a) Snyder, S. A.; Breazzano, S. P.; Ross, A. G.; Lin, Y. Q.; Zografos, A. L. *J. Am. Chem. Soc.* **2009**, *131*, 1753-1765; b) Jia, Y.; Li, T.; Yu, C.; Jiang, B.; Yao, C. *Org. Biomol. Chem.* **2016**, *14*, 1982-1987; c) Matsuura, B. S.; Keylor, M. H.; Li, B.; Lin, Y.; Allison, S.; Pratt, D. A.; Stephenson, C. R. J. *Angew. Chem.* **2015**, *127*, 3825-3828.
- [17] a) Jeffrey, J. L.; Sarpong, R. *Org. Lett.* **2009**, *11*, 5450-5453; b) Klotter, F.; Studer, A. *Angew. Chem., Int. Ed.* **2014**, *53*, 2473-2476; c) Kim, I.; Choi, J. *Org. Biomol. Chem.* **2009**, *7*, 2788-2795; d) Kim, K.; Kim, I. *Org. Lett.* **2010**, *12*, 5314-5317.

- [18] Li, C.; Lu, J.; Xu, X.; Hu, R.; Pan, Y. *Green Chemistry* **2012**, *14*, 3281-3284.
- [19] Kurosawa, W.; Kan, T.; Fukuyama, T. *J. Am. Chem. Soc.* **2003**, *125*, 8112-8113.
- [20] Koizumi, Y.; Kobayashi, H.; Wakimoto, T.; Furuta, T.; Fukuyama, T.; Kan, T. *J. Am. Chem. Soc.* **2008**, *130*, 16854-16855.
- [21] Wakimoto, T.; Miyata, K.; Ohuchi, H.; Asakawa, T.; Nukaya, H.; Suwa, Y.; Kan, T. *Org. Lett.* **2011**, *13*, 2789-2791.
- [22] Wang, D.-H.; Yu, J.-Q. *J. Am. Chem. Soc.* **2011**, *133*, 5767-5769.
- [23] Javed, M. I.; Brewer, M. *Org. Synth.* **2008**, *85*, 189-195.
- [24] a) Morrison, H.; Yates, P.; Danishefsky, S. J. *Org. Chem.* **1961**, *26*, 2617-2618; b) Severin, T.; Pehr, H. *Chem. Ber.* **1979**, *112*, 3559-3565.
- [25] For precedent for the formation of azines in Rh-catalyzed reactions of diazocompounds, see Panish, R.; Selvaraj, R.; Fox, J. M. *Org. Lett.* **2015**, *17*, 3978-3981, and references therein.
- [26] Computations were carried out using Gaussian09 (Frisch, M. J., et al.; Gaussian, Inc. : Wallingford, CT, 2009; full reference in Supporting Information) and the B3LYP functional (A. D. Becke, *J. Chem. Phys.* **1993**, *98*, 1372-1377; A. D. Becke, *J. Chem. Phys.* **1993**, *98*, 5648-5652; C. Lee, W. Yang, R. G. Parr, *Phys. Rev. B* **1988**, *37*, 785-789; P. J. Stephens, F. J. Devlin, C. F. Chabalowski, M. J. Frisch, *J. Phys. Chem.* **1994**, *98*, 11623-11627; J. Tirado-Rives, W. L. Jorgensen, *J. Chem. Theory Comput.* **2008**, *4*, 297-306), along with the 6-31G(d) basis set for C, H, N and O and the LANL2DZ basis set for Rh. Energies discussed in the text are free energies at 298K.
- [27] Davies, H. M. L.; Beckwith, R. E. *J. Chem. Rev.* **2003**, *103*, 2861-2904
- [28] Taber, D. F.; Guo, P. *J. Org. Chem.* **2008**, *73*, 9479-9481
- [29] Quiclet-Sire, B.; Zard, S. Z. *Chem. Commun.* **2006**, 1831-1832.
- [30] a) Slates, H. L.; Wendler, N. L. *J. Am. Chem. Soc.* **1959**, *81*, 5472-5475; b) Kocsis, K.; Ferrini, P. G.; Arigoni, D.; Jeger, O. *Helv. Chim. Acta* **1960**, *43*, 2178-2181; c) Adam, W.; Diederling, M.; Trofimov, A. V. *J. Phys. Org. Chem.* **2004**, *17*, 643-655.
- [31] See supporting information.
- [32] Nakamura, E.; Yoshikai, N.; Yamanaka, M. *J. Am. Chem. Soc.* **2002**, *124*, 7181-7192.
- [33] a) Taber, D. F.; You, K. K.; Rheingold, A. L. *J. Am. Chem. Soc.* **1996**, *118*, 547-556; b) Hare, S. R.; Tantillo, D. J. *Chem. Sci.* **2017**, *8*, 1442-1449..
- [34] a) Nowlan, D. T.; Singleton, D. A. *J. Am. Chem. Soc.* **2005**, *127*, 6190-6191; b) DeAngelis, A.; Dmitrenko, O.; Yap, G. P. A.; Fox, J. M. *J. Am. Chem. Soc.* **2009**, *131*, 7230-7231; c) DeAngelis, A.; Dmitrenko, O.; Fox, J. M. *J. Am. Chem. Soc.* **2012**, *134*, 11035-11043.
- [35] Panish, R.; Chintala, S. R.; Boruta, D. T.; Fang, Y.; Taylor, M. T.; Fox, J. M. *J. Am. Chem. Soc.* **2013**, *135*, 9283-9286.
- [36] Miller, S. R.; Krasutsky, S.; Kiprof, P. J. *Mol. Struct. (Theochem)* **2004**, *674*, 43-47
- [37] DeAngelis, A.; Dmitrenko, O.; Yap, G. P. A.; Fox, J. M. *J. Am. Chem. Soc.* **2009**, *131*, 7230-7231
- [38] Werlé, C.; Goddard, R.; Philipps, P.; Farès, C.; Fürstner, A. *Angew. Chem., Int. Ed.* **2016**, *55*, 10760-10765
- [39] DeAngelis, A.; Dmitrenko, O.; Yap, G. P. A.; Fox, J. M. *J. Am. Chem. Soc.* **2009**, *131*, 7230-7231
- [40] a) Nishio, M. *PCCP* **2011**, *13*, 13873-13900; b) Takahashi, O.; Kohno, Y.; Nishio, M. *Chem. Rev.* **2010**, *110*, 6049-6076; c) Steiner, T. *Angew. Chem., Int. Ed.* **2002**, *41*, 48-76.
- [41] DeAngelis, A. (2011). Rhodium(II)-catalyzed intermolecular reactions of α -alkyl- α -diazooesters: Selectivity over β -hydride elimination (Doctoral dissertation).
- [42] Melník, M.; Progress in Coordination and Bioinorganic Chemistry; Slovak Techn. University Press, **2003**, 213.
- [43] Hashimoto, S.; Watanabe, N.; Ikegami, S. *Tetrahedron Lett.* **1992**, *33*, 2709-2712.